

Slope-Mass-Correlation in Diffractive Dissociation Reactions

A.C.B. ANTUNES

Instituto de Física, Universidade Federal da Rio de Janeiro, Caixa Postal 68528, Rio de Janeiro, 21910, RJ, Brasil

and

A.F.S. SANTORO and M.H.G. SOUZA

Centro Brasileiro de Pesquisas Físicas, Rua Dr. Xavier Sigaud 150, Rio de Janeiro, 22290. RJ, Brasil

Recebido em 26 de Dezembro de 1984

Abstract We present in this paper a set of new results of new Three Component Deck Model for Diffractive Dissociation Reactions. These new results are confronted with recently published ones to obtain a general view of the model, its predictions and comparison with experimental results. Two kinds of correlations and amplitudes are given: the slope-mass-cos θ_{GJ} and slope-mass-partial wave correlations.

1. INTRODUCTION

One of the most important parts of high energy scattering is the Inelastic diffractive component or diffraction dissociation. The Three Component Deck Model (TCDM) gives a very good description of the diffractive dissociation phenomena. We have made¹ applications of the model to several reactions, with very good results. Other applications are presented in the present paper, giving a certain universalization to the model. In this paper we confront the previous results with the new applications of the TCDM, exhibiting a general view of its main properties. For a general review of all diffractive aspects of scattering, see reference 2.

Similarly to other aspects of the scattering process, the inelastic part has also soft and hard components in the physical regions. While the soft component has been very much studied and is described by good models, the hard component appears at high energies and very large momentum transfers, and is due to the interactions of the hadron constituents. It is an open subject.

In this paper we limit ourselves to the diffractive dissociation soft component and specifically to the TCDM^{1a}. We have shown¹

that this model reproduces the main aspects of the diffractive dissociation reactions (DDR). Here, we put together all new and published results for different reactions, giving a systematic description of the spin-parity structure. The TCDM is the only model describing, among the main properties of the data, the mass-slope-cos θ_{GJ} and mass-slope-partial-wave correlations. A summary of the improvements, derivations, spin-parity structures for each reaction, approximations and hypotheses are given in the next sections. Section 2 is dedicated to the model and the main aspects of its derivation. In section 3 we give the applications of the TCDM to several reactions with different spin and parity structure in the $a + P \rightarrow i + 2$ subreaction (here a is the beam-particle, P is the Pomeron exchanged in the complete inelastic reaction and $1 + 2$ represents the subsystem in which we study the effective mass distributions and general properties). Partial wave amplitudes for each reaction are given in section 4. Finally in section 5 we present the discussion and conclusions from our study.

2. THREE COMPONENTS DECK MODEL

We present now the general description, properties and main parts of the derivations of the TCDM.

In all cases, we have considered a general reaction $a+b \rightarrow (1+2)+3$, see fig.1, where $b = 3 = \text{nucleon}$, at very high energy, where the diffractive phenomena are dominant. In TCDM the diffractive character is represented by the Pomeron (P) exchange. The dissociation of the hadron (a) into a pair $(1+2)$ is described by the coherent sum of the Born terms of the exchange amplitudes of the (a) , (1) and (2) particles or the s , u and t channel respectively of the subreaction $a + P \rightarrow 1 + 2$ (see fig. 2). We use a standard parametrization of the Pomeron exchange, as described below. The two parameters b and σ_p , the slope and the high energy

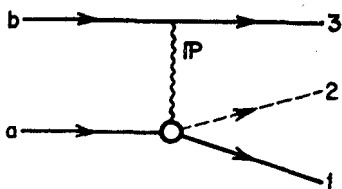


Fig.1 - Single Pomeron exchange in the $a + b \rightarrow (1 + 3) + 2$ reaction at high energy.

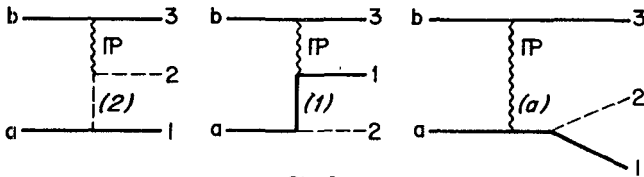


Fig. 2

Fig.2 - The three components of the (TDCM), representing the t_1 -channel, u_1 -channel and s_1 -channel of the $a + b \rightarrow (1+2) + 3$ reaction.

total cross section are in general experimentally known. But in our case the subreactions $(2) + (b) \rightarrow (2) + (3=b)$, $(1) + (b) \rightarrow (1) + (3=b)$ and $(a) + (b) \rightarrow (a) + (3=b)$ are off-mass-shell in the sense that (2) , (1) and (a) are off-mass-shell particles. Then we must correct the off-shell problem by changing slightly the b and σ_T in each case. This is the best way to consider indirectly a form factor without breaking some other important properties, as the interferences among the three terms.

The well known Gribov-Morrison rule³, $\Delta P = (-1)^{\Delta J}$, where ΔP and ΔJ are the parity and spin balance between the particles in the diffractive vertex, is automatically satisfied in elastic diffractive subreactions, which appear in the TDCM.

To obtain the hadronic current coupled to the Pomeron, in TDCM we assume the vector coupling hypothesis (VCH). On the current constructed with this hypothesis we impose the s-channel helicity conservation (SCHC)⁴, which simplifies the form of the coupling, and reduces the coupling constants to only one. It is a well known experimental result that in the elastic diffractive reactions, dominated by the Pomeron exchange, the Pomeron couples only to the s-channel helicity conserving hadronic vertex.

In the high energy approximation (HEA), defined in Appendix A the current, for a vertex $a(p, \lambda) b(p', \lambda')$ obtained with (VCH), has the general form⁵

$$J_{\lambda', \lambda}^{\beta} (p', p) \simeq (-t)^{|\lambda' - \lambda|/2} V(\lambda', \lambda) P^{\beta} \quad (1)$$

where $t = (p' - p)^2$, $P = (p' + p)/2$ and $V(\lambda', \lambda)$ are functions of the coupling constants, the masses m_a , m_b and the momentum transfer t .

Imposing the SCHC on these currents, they become^{1d}

$$J_{\lambda',\lambda}^{\beta}(p',p) \simeq 2g_a \mathbf{P} b P^{\beta} \delta_{\lambda',\lambda} \quad (2)$$

In the diffractive region, dominated by the Pomeron exchange, the helicity amplitudes are essentially imaginary. For a generic diffractive reaction,

$$a(p, \lambda_a) + b(q, \lambda_b) \rightarrow a(p', \lambda'_a) + b(q', \lambda'_b)$$

the helicity amplitudes may be written as

$$A(s,t)_{\lambda_a, \lambda_b, \lambda'_a, \lambda'_b} = \frac{i}{2} e^{Bt/2} J_{\beta; \lambda'_a \lambda_a} J_{\lambda'_b \lambda_b}^{\beta} \quad (3)$$

The relation among the coupling constants, which appear in the currents, and the total cross section is given by the optical theorem

$$g_{a\mathbf{P}} g_{b\mathbf{P}} = \sigma_{\text{Tot}}^{ab}(s) \quad (4)$$

Off mass shell corrections must be introduced in the diffractive amplitudes contained in the TCDM. It is important to emphasize the inconvenience of introducing new form factors to take into account off mass shell effects. The complications due to the presence of these form factors could destroy the possible interferences among the components of TCDM.

The most convenient way to introduce the off-mass shell effects is via small variations of the experimental diffractive slopes (B_{2b}, B_{1b} and B_{ab}) and the cross section values ($\sigma_{\text{Tot}}^{2b}(s_2), \sigma_{\text{Tot}}^{1b}(s_3)$ and $\sigma_{\text{Tot}}^{ab}(s)$).

In the HEA, the general form of the common vertex $b\mathbf{P}3$, considering that $b = 3$, is given by

$$J_{\lambda_3 \lambda_b}^{\beta} \simeq 2g_{b\mathbf{P}} R^{\beta} \delta_{\lambda_3 \lambda_b} \quad (5)$$

where $R = (p_b + p_3)/2$.

The factorization property of the pomeron permits to factorize this common vertex in the TCDM. This factorization may be represented as in fig. (3).

A consequence of this property in the case of the TCDM is that the spins of the $b\mathbf{P}3$ vertex do not affect the general structure of the TCDM. Then, at the HEA, the spins of the particles b and 3 may be neglected, and the current in eq. (5) may be written as

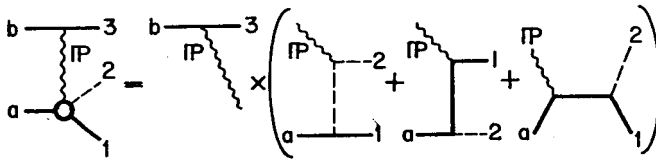


Fig. 3

Fig.3 - Graphical representation of the Pomeron factorization property.

$$J^\beta \sim 2g_{bP} R^\beta \quad (6)$$

To materialize the problem and to introduce a standard notation for our applications of TCDM, let us consider a particular type of reaction in which the particle $b = 3$ is a nucleon and $a, 1$ and 2 are spinless hadrons.

The amplitudes for each component of the TCDM, represented in fig. (2), with the kinematics defined in Appendix A, are

$$A(t) = \frac{i}{2} e^{B_{2b} t_2 / 2} (2g_{bP} R^\beta) (2g_{2P} Q_\beta) \frac{1}{t_1 - m_2^2} g_{a12} \quad (7a)$$

$$A(u) = \frac{i}{2} e^{B_{1b} t_2 / 2} (2g_{bP} R^\beta) (2g_{1P} P_\beta) \frac{1}{u_1 - m_1^2} g_{a12} \quad (7b)$$

and

$$A(s) = \frac{i}{2} e^{B_{ab} t_2} (2g_{bP} R^\beta) (2g_{aP} K_\beta) \frac{1}{s_1 - m_a^2} g_{a12} \quad (7c)$$

To simplify these expressions we define

$$g^t(t_2) = \sigma_{\text{tot}}^{2b}(s_2) e^{B_{2b} t_2 / 2}$$

$$g^u(t_2) = \sigma_{\text{tot}}^{1b}(s_3) e^{B_{1b} t_2 / 2}$$

and

$$g^s(t_2) = \sigma_{\text{tot}}^{ab}(s) e^{B_{ab} t_2 / 2} \quad (8)$$

where, according eq. (4),

$$\sigma_{\text{tot}}^{2b}(s_2) = g_{bP} g_{2P}, \quad \sigma_{\text{tot}}^{1b}(s_3) = g_{bP} g_{1P}$$

and

$$\sigma_{\text{tot}}^{ab}(s) = g_{\text{LP}} g_{\text{CP}}$$

and also

$$T = ig_{\alpha 12} g^t(t_2) / (t_1 - m_2^2)$$

$$U = ig_{\alpha 12} g^u(t_2) / (u_1 - m_1^2) \quad (9)$$

and

$$S = ig_{\alpha 12} g^s(t_2) / (s_1 - m_\alpha^2)$$

At the HEA in eq. (A.9), using eq. (A.10) and the definitions above, the components in eq. (7) become

$$A(t) = T = s_2 \cdot T$$

$$A(u) = U = s_3 \cdot U \quad (10)$$

and

$$A(s) = S = s \cdot S$$

The scattering amplitude is the coherent sum of the three components

$$A = A(s) + A(t) + A(u)$$

Then for reactions with spinless particles in the dissociative vertex,

$$\delta_\alpha = \delta_1 = \delta_2 = 0$$

the TCM yields

$$A = S + T + U = ig_{\alpha 12} \left\{ \frac{s \cdot g^s(t_2)}{s_1 - m_\alpha^2} + \frac{s_2 \cdot g^t(t_2)}{t_1 - m_2^2} + \frac{s_3 \cdot g^u(t_2)}{u_1 - m_1^2} \right\} \quad (11)$$

The general forms of the components, considering the spin factors, are

$$A(s) = F(s) \cdot S, \quad A(t) = F(t) \cdot T$$

and

$$A(u) = F(u) \cdot U$$

where

$$F(s), F(t) \quad \text{and} \quad F(u)$$

are functions of the masses and Invariants in eq. (A.3). It is clear that for spinless particles $F^{(s)} = s$, $F^{(t)} = s_2$ and $F^{(u)} = s_3$.

The components of the TCDM summed up coherently may interfere destructively in some kinematical regions. This interference is the mechanism which gives rise to the correlation among three variables: the diffractive slope B , the effective mass $M_{12} = \sqrt{s_1}$ of the dissociated system, and the polar coordinate θ^{GJ} of a dissociated particle momentum \vec{p}_1 relative to the incident beam momentum \vec{p}_a in the GJS.

Another feature of this correlation is the slope-mass-partial wave correlation, which will be studied in section 4. A direct consequence of the Interferences above mentioned is the large slopes and/or the dips obtained in the $d\sigma/dt_2$ distributions.

In the spinless cases it is possible to obtain relations that give the positions of the dips and show clearly the correlation among M_{12} , $\cos\theta^{GJ}$ and t_2 .

At HEA, $s \simeq s_2 + s_3$, taking this into the eq. (11) and equal to zero the coefficients of s_2 and s_3 , we obtain

$$\begin{aligned} Z_{st} &\equiv g^s(t_2)(t_1 - m_2^2) + g^t(t_2)(s_1 - m_a^2) = 0 \\ Z_{su} &\equiv g^s(t_2)(u_1 - m_1^2) + g^u(t_2)(s_1 - m_a^2) = 0 \end{aligned} \quad (12)$$

Some observations may be made about these equations:

- a) they may be satisfied in the physical region, since in this region $s_1 - m_a^2$ is positive whereas $t_1 - m_2^2$ and $u_1 - m_1^2$ are negative.
- b) they may be rewritten as

$$\begin{aligned} \cos\theta^{GJ} &= f_1(t_2) \\ M_{12} &= f_2(t_2) \end{aligned} \quad (13)$$

which show clearly the correlation among the three variables M_{12} , $\cos\theta^{GJ}$ and t_2 , predicted by this model.

c) the factorization of the elastic vertex hP^3 in the TCDM, according to fig. (3), shows that the position $(M_{12}, \cos\theta^{GJ}, t_2)$ of the zero in the amplitude, or of the dip in $d\sigma/dt_2$, is independent of the hadron b .

d) the parameters that fix the position of the zeros of the amplitudes are the total cross sections $\sigma_{tot}^{ib}(s)$ and the elas-

tic slopes B_{ib} ($i = a, 1, 2$).

Dual Reggeization of TCDM

In the present form of the TCDM, each component is the Born term of the amplitudes for exchange of the particles a, 1 and 2. The validity of the model is restricted to the effective mass $M_{12} = (\sqrt{s_1})$ range between the threshold and the resonances of the dissociated subsystem 1+2.

The need for reggeization has been known since the beginning of the DDR phenomenology development,

The reggeization of the TCDM must be done with some care. The components of exchange of particles a, 1 and 2 must be handled in a symmetric way, because the Interferences that generate the slope-mass-cose^G correlation must not be lost in the course of the process.

The solution of this problem is given by duality, which provides a Regge behaviour for the three channels, avoiding double counting and treating all channels in a symmetric way^{ia}.

The procedure for dual reggeization of the TCDM in the spinless case has been performed^{ia} using the Veneziano formula

$$A = ig_{a12} \left\{ s_3 Z_{su} \frac{\Gamma(-\alpha_s)\Gamma(-\alpha_u)}{\Gamma(1-\alpha_s-\alpha_u)} + s_2 Z_{st} \frac{\Gamma(-\alpha_s)\Gamma(-\alpha_t)}{\Gamma(1-\alpha_s-\alpha_t)} \right\} \quad (14)$$

where

$$a_s = s_1 - m_a^2, \quad \alpha_t = t_1 - m_2^2 \quad \text{and} \quad a_u = u_1 - m_1^2$$

3. APPLICATIONS OF TCDM TO SEVERAL TYPES OF DDR

In this section we collect several results of the applications of TCDM. The DDR studied here have different configurations of spin and parity in the dissociative vertex ($a \rightarrow 1 + 2$). These configurations will be denoted as $s_\alpha^P \rightarrow s_1^P, s_2^P$.

The following configurations are analysed here

$$A - (0^- \rightarrow 0^+, 0^-)$$

$$B - (0^- \rightarrow 1^-, 0^-)$$

$$C - (1/2^+ \rightarrow 1/2^+, 0)$$

and

$$D - (1/2^+ + 3/2^+, 0^-)$$

Some examples of reactions that correspond to these structures of spin and parity are

$$A - \pi + p \rightarrow (\epsilon + a) + p$$

$$K + p \rightarrow (\kappa + \pi) + p$$

$$B - \pi + p \rightarrow (\rho^0 + \pi) + p$$

$$K + p \rightarrow (K^* + \pi) + p$$

$$C - p + p \rightarrow (n + \pi^+) + p$$

$$p + p \rightarrow (\Lambda + K^+) + p$$

$$D - p + p \rightarrow (\Delta^{++} + \pi^-) + p$$

The TCDM amplitudes for DDR of type A have already been obtained in the precedent section.

For reactions of type B, using the kinematics of Appendix A the components of TCDM are

$$A_{\lambda_1}^{(t)} = \frac{i}{2} e^{B_{b2} t_2 / 2} (2g_{bP} R^\beta) (2g_{2P} Q_\beta) \frac{1}{t_1 - m_2^2} g_{a12} \epsilon_\mu^*(p_1, \lambda_1) p_a^\mu$$

$$A_{\lambda_1}^{(s)} = \frac{i}{2} e^{B_{ab} t_2 / 2} (2g_{bP} R^\beta) (2g_{aP} K_\beta) \frac{1}{s_1 - m_a^2} g_{a12} \epsilon_\mu^*(p_1, \lambda_1) p_2^\mu \quad (15)$$

$$A_{\lambda_1}^{(u)} = \frac{i}{2} e^{B_{1b} t / 2} (2g_{bP} R^\beta) \epsilon_\mu^*(p_1, \lambda_1) \Gamma^{\mu\beta\nu} \frac{(-g_{\nu\sigma} + k_\nu k_\sigma / k^2)}{u_1 - m_1^2} g_{a12} (p_{\alpha+p_2})^\sigma / 2$$

where $\epsilon_\mu(p_1, \lambda_1)$ is the wave function for spin 1 particles and

$$\Gamma^{\mu\beta\nu} = 2g_{1P} \left[2(g^{\mu\beta} p^\nu + p^\mu g^{\beta\nu}) - g^{\mu\nu} p^\beta \right] \quad (16)$$

is the s-channel helicity conserving coupling in the vertex $1 \bar{P} 1^-$.

In the HEA, using the notation introduced in section 2, those components may be written as

$$A_{\lambda_1}^{(t)} \sim T \epsilon_\mu^*(p_1, \lambda_1) p_a^\mu$$

$$A_{\lambda_1}^{(s)} \sim S \epsilon_\mu^*(p_1, \lambda_1) p_2^\mu$$

and

$$A_{\lambda_1}^{(u)} \sim \left[U p_\alpha^\mu + s U (p^\mu - p_\alpha^\mu) - U R^\mu (s_1 + m_\alpha^2 - m_2^2 - t_1)/4 \right] \epsilon_\mu^*(p_1, \lambda_1) \quad (17)$$

In the G.J.S. we have

$$p_\alpha^\mu = E_\alpha E^\mu + |\vec{p}_\alpha| Z^\mu \quad \text{and} \quad p^\mu = \sqrt{s_1} E^\mu \quad (18)$$

and for HEA

$$R^\mu \sim \frac{s}{-2\sqrt{s_1}} (E^\mu + \sin \alpha X^\mu + \cos \alpha Z^\mu) \quad (19)$$

where

$$E^\mu = , \quad X^\mu = \begin{pmatrix} 0 \\ 1 \\ 0 \\ 0 \end{pmatrix} \quad \text{and} \quad Z^\mu = \begin{pmatrix} 0 \\ 0 \\ 0 \\ 1 \end{pmatrix} \quad (20)$$

Taking these results into eqs.(17) and summing up the components, the helicity amplitudes read

$$\begin{aligned} A_{\lambda_1} = & \{ \sqrt{s_1} S + E_\alpha T + E_\alpha U + s U (m_1^2 + m_2^2 - m_\alpha^2 + t, -u_1)/4\sqrt{s_1} \} \epsilon_\mu^*(p_1, \lambda_1) E^\mu \\ & + \{ s_2 |\vec{p}_\alpha| \tau + s U [|\vec{p}_\alpha| - (s_1 + m_\alpha^2 - m_2^2 - t_1) \cos \alpha / 4\sqrt{s_1}] \} \epsilon_\mu^*(p_1, \lambda_1) Z^\mu \\ & - [s U (s_1 + m_\alpha^2 - m_2^2 - t_1) \sin \alpha / 4\sqrt{s_1}] \epsilon^*(p_1, \lambda_1) X^\mu \end{aligned} \quad (21)$$

The spin 1 wave functions are

$$\epsilon^{\mu*}(p_1, 0) = \frac{1}{m_1} \begin{pmatrix} p_1 \\ E_1 \sin \theta \cos \phi \\ E_1 \sin \theta \sin \phi \\ E_1 \cos \theta \end{pmatrix} \quad (22)$$

$$\epsilon^{\mu*}(p_1, \pm 1) = \frac{e^{\mp i \phi}}{\sqrt{2}} \begin{pmatrix} 0 \\ \mp \cos \theta \cos \phi - i \sin \phi \\ \cos \theta \sin \phi + i \cos \phi \\ \pm \sin \theta \end{pmatrix}$$

and the helicity amplitudes in eq. (21) are written explicitly

$$\begin{aligned}
A_{\lambda_1=0} = & |\vec{p}_1| \{ \sqrt{s_1} S + E_\alpha T + E_\alpha U + s U (m_1^2 + m_2^2 - m_\alpha^2 + \\
& + t_2 - u_1) / 4\sqrt{s_1} \} / m_1 - E_1 \{ s_2 |\vec{p}_\alpha| T + s U [|\vec{p}_\alpha| - (s_1 \\
& + m_\alpha^2 - m_2^2 - t_1) \cos \alpha / 4\sqrt{s_1}] \} \cos \theta / m_1 - s U E_1 (s_1 + m_\alpha^2 \\
& - m_2^2 - t_1) \sin \alpha \sin \theta \cos \phi / (4m_1 \sqrt{s_1})
\end{aligned} \tag{23}$$

and

$$\begin{aligned}
A_{\lambda_1=\pm 1} = & \mp e^{\mp i\phi} \{ \{ s_2 |\vec{p}_\alpha| T + s U [|\vec{p}_\alpha| - (s_1 + m_\alpha^2 - m_2^2 \\
& - t_1) \cos \alpha / 4\sqrt{s_1}] \} \sin \theta - s U (s_1 + m_\alpha^2 - m_2^2 - \\
& - t_1) \sin \alpha (\cos \theta \cos \phi \pm i \sin \phi) / 4\sqrt{s_1} \} / \sqrt{2}
\end{aligned} \tag{24}$$

The possible zeros in these amplitudes may not be determined by simple equations like those for spinless reactions. In this case, the zeros must be found numerically.

Reactions of type C have the following components for the TCDM

$$\begin{aligned}
A_{\lambda_1 \lambda_\alpha}^{(t)} &= 2TR \bar{Q} \bar{u}(p_1, \lambda_1) \gamma_5 u(p_\alpha, \lambda_\alpha) \\
A_{\lambda_1 \lambda_\alpha}^{(u)} &= U \bar{u}(p_1, \lambda_1) \not{k} (k + m_1) \gamma_5 u(p_\alpha, \lambda_\alpha)
\end{aligned} \tag{25}$$

and

$$A_{\lambda_1 \lambda_\alpha}^{(s)} = S \bar{u}(p_1, \lambda_1) \gamma_5 (\not{p} + m_\alpha) \not{u}(p_\alpha, \lambda_\alpha)$$

The helicity amplitudes, obtained summing these components, may be written as

$$A_{\lambda_1 \lambda_\alpha} = R_\beta \bar{u}(p_1, \lambda_1) \{ 2(T + S) p_2^\beta \gamma_5 - (U + S) \gamma^\beta \not{p}_2 \gamma_5 \} u(p_\alpha, \lambda_\alpha) \tag{26}$$

where we have assumed $m_1 = m_\alpha$.

There may occur zeros in these amplitudes, due to interferences among the components, if

$$T + S = 0 \quad \text{and} \quad U + S = 0 \tag{27}$$

in the physical region. The equations for the zeros are

$$Z_{st} = (s_1 - m_\alpha^2)g^t(t_2) + (t_1 - m_\pi^2)g^s(t_2) = 0 \quad (28)$$

$$Z_{su} = (s_1 - m_\alpha^2)g^u(t_2) + (u_1 - m_\pi^2)g^s(t_2) = 0$$

These equations are the same as those (eq.(12)) obtained for *spinless* reactions.

For the reaction $\bar{p}p \rightarrow n \pi p$, ^{1a}, from eqs. (28) and using the relation

$$s_1 + t_1 + u_1 = 2m_N^2 + m_\pi^2 + t_2$$

we obtain

$$t_1(d|p) = m_\pi^2 + t_2$$

and

$$s_1(d|p) = m_N^2 - t_2 \cdot e^{\frac{\Delta \cdot t_2}{2}} \cdot \delta \quad (29)$$

where

$$\delta = \sigma_{NN}/\sigma_{\pi N} \quad \text{and} \quad A = (B_{NN} - B_{\pi N})/2$$

These equations describe correctly the behaviour of the zero in the amplitudes, or the dip in $d\sigma/dt_2$.

The helicity amplitudes for this type of reaction may be written in a form more convenient for calculations. Summing the components in eq. (25), we obtain in the HEA

$$A_{\lambda_1 \lambda_\alpha} = (S + T + U) \bar{u}(p_1 \lambda_1) \gamma_5 u(p_\alpha \lambda_\alpha) - i s |\vec{p}_\alpha| (S+U) \sin \alpha \bar{u}(p_1 \lambda_1) (\sigma^{31} - \cos \alpha \sigma^{01} + \sin \alpha \sigma^{03}) \gamma_5 u(p_\alpha \lambda_\alpha) / 2\sqrt{s_1} \quad (30)$$

This gives explicitly

$$A_{\pm 1/2, \pm 1/2} = \pm \{ (S + T + U) G_- \cos(\theta/2) - s |\vec{p}_\alpha| (S+U) \sin \alpha [\bar{E}_+ \sin \alpha \cos(\theta/2) - e^{+i\phi} (G_+ + E_+ \cos \alpha) \sin(\theta/2)] / 2\sqrt{s_1} \} \quad (31)$$

and

$$\begin{aligned}
 A_{\pm 1/2, \pm 1/2} = & -e^{\pm i\phi} \cdot \{ (S + T + U) G_{\pm} \sin(\theta/2) \\
 & + s | \vec{p}_{\alpha} | \{ (S+U) \sin a [E_{-} \sin a \sin(\theta/2) - e^{-i\phi} (\cos a \cos(\theta/2))] / 2\sqrt{s_1} \} \\
 & + E_{-} \cos a \cos(\theta/2) \} / 2\sqrt{s_1} \} \quad (32)
 \end{aligned}$$

where

$$\begin{aligned}
 E_{\pm} &= (E_1 + m_1)^{1/2} (E_a + m_a)^{1/2} \pm (E_1 - m_1)^{1/2} (E_a - m_a)^{1/2} \\
 G_{\pm} &= (E_1 + m_1)^{1/2} (E_a - m_a)^{1/2} \pm (E_1 - m_1)^{1/2} (E_a + m_a)^{1/2}
 \end{aligned} \quad (33)$$

Dual Resonance Parametrization

The TCOM for the reactions of type C may be reggeized and dualized. The helicity amplitudes in eq. (26) may be written as

$$A_{\lambda_1 \lambda_2} = \bar{u}(p_1 \lambda_1) \left\{ \frac{2R \cdot p_2^z \gamma_5}{(s_1 - m_a^2)(t_1 - m_2^2)} - \frac{Z_{su} \not{p}_2 \gamma_5}{(s_1 - m_a^2)(u_1 - m_1^2)} \right\} u(p_2 \lambda_2) \quad (34)$$

The prescription for dual resonance parametrization (DRP) consists in performing in eq. (34) the substitutions

$$1 / (s_1 - m_a^2) (t_1 - m_2^2) \rightarrow \frac{\Gamma(-\alpha_a(s_1)) \Gamma(-\alpha_2(t_1))}{\Gamma(1 - \alpha_a(s_1) - \alpha_2(t_1))} \quad (35)$$

and

$$1 / (s_1 - m_a^2) (u_1 - m_1^2) \rightarrow \frac{\Gamma(-\alpha_a(s_1)) \Gamma(-\alpha_1(u_1))}{\Gamma(1 - \alpha_a(s_1) - \alpha_1(u_1))} \quad (36)$$

The Regge trajectories are parametrized by

$$\alpha_1(u_1) = u_1 - m_1^2, \quad \alpha_2(t_1) = t_1 - m_2^2 \quad (37)$$

and

$$\alpha_a(s_1) = s_1 - m_a^2 + i h (s_1 - (m_1 + m_2)^2)^{1/2}$$

where the parameter h controls the resonance width.

The TCOM has been applied to the reaction $pp \rightarrow A^+ \pi^- p$, which is of type D. Its amplitudes are given in reference 1d.

4. PARTIAL WAVE AMPLITUDES

In this section we project the helicity amplitudes, obtained in section 3, into partial waves.

For reactions of type A, ($0^- \rightarrow 0^+, 0^-$), the partial wave amplitudes are given by eq. (B.5), for $\lambda_\alpha = 0$ and $N_{12} = -1$. We then have

$$A^{JM, -} = ((2J + 1)/4\pi)^{1/2} \int d\Omega e^{-iM\phi} a_{M0}^J(\theta) A(\theta, \phi)$$

and

$$A^{JM, +} = 0 \quad (38)$$

and the parity of these amplitudes is $P = -(-1)^J$.

The amplitude $A(\theta, \phi)$, given by eq. (11), may be written as

$$A(\theta, \phi) = A^{(1)}(\theta) + A^{(2)}(\theta) \cdot \cos\phi \quad (39)$$

where

$$A^{(1)}(\theta) = ig_{\alpha 12} [sg^s(t_2)/(s_1 - m_\alpha^2) + a_2 g^t(t_2)/(t_1 - m_2^2) + a_3 g^u(t_2)/(u_1 - m_1^2)] \quad (40)$$

$$A^{(2)}(\theta) = ig_{\alpha 12} b [g^t(t_2)/(t_1 - m_2^2) - g^u(t_2)/(u_1 - m_1^2)] \quad (41)$$

For HEA we have

$$\begin{aligned} a_2 &\simeq s(E_2 + |\vec{p}_1| \cos\alpha \cos\theta) \sqrt{s_1} \\ a_3 &\simeq s(E_1 - |\vec{p}_1| \cos\alpha \cos\theta) / \sqrt{s_1} \end{aligned} \quad (42)$$

and

$$b \simeq s |\vec{p}_1| \sin\alpha \sin\theta / \sqrt{s_1}$$

The Integration over ϕ shows that there are non-vanishing amplitudes only for $M=0$ and $M=\pm 1$, and that

$$A^{J, M = -1, -} = -A^{J, M = +1, -}$$

We introduce the notation

$$A\left(\begin{smallmatrix} L \\ J \end{smallmatrix}\right)_M^P = A^{J, M, -} \quad (43)$$

where $J=L$, and the S, P and D partial wave amplitudes are given by

$$\begin{aligned}
A(S_0^-)_0 &= \pi^{1/2} \int_{-1}^1 d(\cos \theta) d_{00}^0(\theta) A^{(1)}(\theta) \\
A(P_1^+)_0 &= (3\pi)^{1/2} \int_{-1}^1 d(\cos \theta) d_{00}^1(\theta) A^{(1)}(\theta) \\
A(P_1^+)_1 &= ((3\pi)^{1/2}/2) \int_{-1}^1 d(\cos \theta) d_{10}^1(\theta) A^{(2)}(\theta) \\
A(D_2^-)_0 &= (5\pi)^{1/2} \int_{-1}^1 d(\cos \theta) d_{00}^2(\theta) A^{(1)}(\theta) \\
A(D_2^-)_1 &= ((5\pi)^{1/2}/2) \int_{-1}^1 d(\cos \theta) d_{10}^2(\theta) A^{(2)}(\theta)
\end{aligned} \tag{44}$$

for reactions of type B ($0^- \rightarrow 1^-, 0^-$), the helicity amplitudes in eqs. (23) and (24) have the form (see eq. B.1)

$$A_{\lambda_1}(\theta, \phi) = e^{-i\lambda_1} \tilde{A}_{\lambda_1}(\theta, \phi) \tag{45}$$

and the partial wave amplitudes are given by eqs. (B.2) and (B.5), for $\lambda_a = \lambda_2 = 0$ and $N_{12} = -1$:

$$A_{\lambda_1}^{JM, \pm} = ((2J+1)/8\pi)^{1/2} \int d\Omega e^{-iM\phi} \{d_{M\lambda_1}^J(\theta) \tilde{A}_{\lambda_1}(\theta, \phi) \mp d_{M, -\lambda_1}^J(\theta) \tilde{A}_{-\lambda_1}(\theta, \phi)\} \tag{46}$$

for $\lambda_1 = \pm 1$

$$A_{\lambda_1}^{JM, -} = ((2J+1)/4\pi)^{1/2} \int d\Omega e^{-iM\phi} d_{M0}^J(\theta) A_0(\theta, \phi) \tag{47}$$

and

$$A_{\lambda_1}^{JM, +} = 0 \quad \text{for } \lambda_1 = 0$$

The parities of these amplitudes are given by

$$P = \pm (-1)^J$$

From eqs. (23) and (24) we see that the expressions for $\tilde{A}_{\lambda_1}(\theta, \phi)$ have the form

$$\tilde{A}_{\lambda_1}(\theta, \phi) = A_{\lambda_1}^{(1)}(\theta) + A_{\lambda_1}^{(2)}(\theta) \cos \phi + A_{\lambda_1}^{(3)}(\theta) \sin \phi \tag{48}$$

where, $A_0^{(3)}(\theta) = 0$, for $h_1 = 0$ and $A_{-1}^{(1)}(\theta) = -A_1^{(1)}(\theta)$ and $A_{-1}^{(2)}(\theta) = -A_1^{(2)}(\theta)$ for $\lambda_1 = \pm 1$. The coefficients $A_{\lambda_1}^{(i)}(\theta)$ ($i = 1, 2, 3$) may be obtained from eqs. (23) and (24).

The integrations on ϕ in eqs. (54) and (55) show that only the values $M=0$ and $M=\pm 1$ correspond to non-vanishing amplitudes.

As we are seeking for possible interferences among the components of TCDM, we choose $M=0$, which selects the coefficients $A_{\lambda_1}^{(1)}(\theta)$. The coefficient $A_0^{(1)}(\theta)$ is the only one that contains the three components of TCDM, and is the more probable to give rise to strong interferences.

From eqs. (54) and (55) we obtain, for $M=0$

$$A_{\lambda_1=0}^{J,M=0,-} = (\pi(2J+1))^{1/2} \int_{-1}^1 d(\cos\theta) d_{00}^J(\theta) A_0^{(1)}(\theta) \quad (49)$$

$$A_{\lambda_1=1}^{J,M=0,-} = (2\pi(2J+1))^{1/2} \int_{-1}^1 d(\cos\theta) d_{01}^J(\theta) A_1^{(1)}(\theta) \quad (50)$$

$$A_{\lambda_1=-1}^{J,M=0,-} = A_{\lambda_1=1}^{J,M=0,-}$$

and

$$A_{\lambda_1}^{J,M=0,+} = 0$$

The amplitudes for well defined orbital angular momentum are given by eq. (B.10). Using the notation

$$A(L_J^P) = A_{(L)}^{J,M=0} \quad (51)$$

the S , P and D partial wave amplitudes are, for $M=0$

$$A(S_1^+) = (1/3)^{1/2} (2A_{\lambda_1=1}^{J=1,M=0,-} + A_{\lambda_1=0}^{J=1,M=0,-})$$

$$A(P_0^-) = -A_{\lambda_1=0}^{J=0,M=0,-}$$

$$A(P_2^-) = (2/5)^{1/2} (\sqrt{3} A_{\lambda_1=1}^{J=2,M=0,-} + A_{\lambda_1=0}^{J=2,M=0,-}) \quad (52)$$

$$A(D_1^+) = (2/3)^{1/2} (A_{\lambda_1=1}^{J=1,M=0,-} - A_{\lambda_1=0}^{J=1,M=0,-})$$

$$A(D_3^+) = (1/7)^{1/2} (2\sqrt{2} A_{\lambda_1=1}^{J=3,M=0,-} + \sqrt{3} A_{\lambda_1=0}^{J=3,M=0,-})$$

The helicity amplitudes for reactions of type C also factorize similarly to eq.(B.1). The partial wave amplitudes are given by eq.(B.2), for $\lambda_2 = 0$ and $N_{12} = -1$ as

$$A_{\lambda_1 \lambda_\alpha}^{JM, \pm} = ((2J+1)/8\pi)^{1/2} \int d\Omega e^{-i(M-\lambda_\alpha)\phi} \{ d_{M \lambda_1}^J(\theta) \tilde{A}_{\lambda_1 \lambda_\alpha}(\theta, \phi) \mp d_{M, -\lambda_1}^J(\theta) \tilde{A}_{-\lambda_1, \lambda_\alpha}(\theta, \phi) \} \quad (53)$$

and the parities of these amplitudes are

$$P = \pm (-1)^{J-1/2} \quad (54)$$

From the helicity amplitudes shown in eqs. (31) and (32) we see that

$$\tilde{A}_{\lambda_1 \lambda_\alpha}(\theta, \phi) = A_{\lambda_1 \lambda_\alpha}^{(1)}(\theta) + A_{\lambda_1 \lambda_\alpha}^{(2)}(\theta) \cdot \cos \phi + A_{\lambda_1 \lambda_\alpha}^{(3)}(\theta) e^{-i2\lambda_\alpha \phi} \quad (55)$$

where the coefficients $A_{\lambda_1 \lambda_\alpha}^{(i)}(\theta)$ may be obtained from those amplitudes.

The Integration on ϕ shows that the non-vanishing amplitudes correspond to $M = \pm \lambda_\alpha$ and $M = \lambda_\alpha \pm 1$. We choose $M = \lambda_\alpha$ because this condition selects the coefficients $A_{\lambda_1 \lambda_\alpha}^{(1)}(\theta)$. Only these coefficients contain the three components of TCDM, and are the most probable source of the interferences we are seeking for. From eqs. (62) and (64) we obtain for $M=\lambda_\alpha$ that

$$A_{\lambda_1 \lambda_\alpha}^{J, M=\lambda_\alpha, \pm} = (\pi(J+1/2))^{1/2} \int_{-1}^1 d(\cos\theta) [d_{\lambda_\alpha \lambda_1}^J(\theta) A_{\lambda_1 \lambda_\alpha}^{(1)} \mp d_{\lambda_\alpha, -\lambda_1}^J(\theta) A_{-\lambda_1, \lambda_\alpha}^{(1)}(\theta)] \quad (56)$$

The partial wave amplitudes for well defined orbital angular momentum L , according to eq. (8.10), are

$$A_{(L=J-1/2)\lambda_\alpha}^{J, M=\lambda_\alpha, -} = 2(2J/(2J+1))^{1/2} C_{0, 1/2, 1/2}^{J-1/2, 1/2, J} A_{1/2, \alpha}^{J, M=\lambda_\alpha, -}$$

$$A_{(L=J+1/2)\lambda_\alpha}^{J, M=\lambda_\alpha, +} = 2(2(J+1)/(2J+1))^{1/2} C_{0, 1/2, 1/2}^{J+1/2, 1/2, J} A_{1/2, \alpha}^{J, M=\lambda_\alpha, +}$$

$$A_{(L=J-1/2)\lambda_\alpha}^{J,M=\lambda_\alpha,+} = 0$$

and

$$A_{(L=J+1/2)\lambda_\alpha}^{J,M=\lambda_\alpha,-} = 0 \quad (57)$$

and satisfy the relations

$$A_{(L=J\pm 1/2),-1/2}^{J,-1/2,\pm} = \pm A_{(L=J\pm 1/2),1/2}^{J,1/2,\pm} \quad (58)$$

Introducing the notation

$$A(L_J^P)_{1/2} \equiv A_{(L)1/2}^{J,M=1/2,\pm} \quad (59)$$

the S , P and D for $M = \lambda_\alpha = 1/2$, are written

$$\begin{aligned} A(S_{1/2}^-)_{1/2} &= \sqrt{2} A_{\lambda_1=1/2, \lambda_\alpha=1/2}^{J=1/2, M=1/2, -} \\ A(P_{1/2}^+)_{1/2} &= -\sqrt{2} A_{\lambda_1=1/2, \lambda_\alpha=1/2}^{J=1/2, M=1/2, +} \\ A(P_{3/2}^+)_{1/2} &= \sqrt{2} A_{\lambda_1=1/2, \lambda_\alpha=1/2}^{J=3/2, M=1/2, -} \\ A(D_{3/2}^-)_{1/2} &= -\sqrt{2} A_{\lambda_1=1/2, \lambda_\alpha=1/2}^{J=3/2, M=1/2, +} \\ A(D_{5/2}^-)_{1/2} &= \sqrt{2} A_{\lambda_1=1/2, \lambda_\alpha=1/2}^{J=5/2, M=1/2, -} \end{aligned} \quad (60)$$

The partial wave amplitudes for reactions of type $D_\alpha(1/2^+ \rightarrow 3/2^+, 0^-)$, are given by^{1d}

$$\begin{aligned} A(S_{3/2}^-)_{1/2} &= A_{3/2,1/2}^{3/2,1/2,+} + A_{1/2,1/2}^{3/2,1/2,+} \\ A(P_{1/2}^+)_{1/2} &= -\sqrt{2} A_{1/2,1/2}^{1/2,1/2} \\ A(P_{3/2}^+)_{1/2} &= -(1/5)^{1/2} (3 A_{3/2,1/2}^{3/2,1/2,-} + A_{1/2,1/2}^{3/2,1/2,-}) \end{aligned}$$

$$\begin{aligned}
A(P_{5/2}^+)_{1/2} &= (1/5)^{1/2} (2 A_{3/2,1/2}^{5/2,1/2,+} + \sqrt{6} A_{1/2,1/2}^{5/2,1/2,+}) \\
A(D_{1/2}^-)_{1/2} &= \sqrt{2} A_{1/2,1/2}^{1/2,1/2,-} \\
A(D_{3/2}^-)_{1/2} &= A_{3/2,1/2}^{3/2,1/2,+} - A_{1/2,1/2}^{3/2,1/2,+} \\
A(D_{5/2}^-)_{1/2} &= -(2/7)^{1/2} (\sqrt{6} A_{3/2,1/2}^{5/2,1/2,-} + A_{1/2,1/2}^{5/2,1/2,-}) \\
A(D_{7/2}^-)_{1/2} &= (1/7)^{1/2} (\sqrt{5} A_{3/2,1/2}^{7/2,1/2,+} + 3 A_{1/2,1/2}^{7/2,1/2,+})
\end{aligned}
\tag{61}$$

5. RESULTS AND DISCUSSIONS

In this paper we analyse the TCDM applications to several types of (DDR). We put together all spin-parity structures of the subreaction $a + P \rightarrow 1 + 2$. These amplitudes can be useful for a complete understanding to the DDR phenomenology. In this sense the model is universal, describing the multiple aspects of the data. The TCDM is a natural consequence of the earlier Drell-Haida-Deck-Model⁶. This model described the DDR until the discovery of the slope (B), mass (M_{12}), angular ($\cos \theta^{G,J}$) and the slope-mass-partial waves correlations.

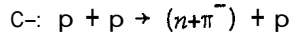
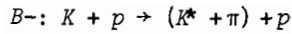
The application of TCDM to these different types of reactions permits us to test the model in those reactions for which there are experimental results, and to give a theoretical prediction for the others.

The DDR studied here have different spin and parity structures in the subreactions ($a + P \rightarrow 1 + 2$).

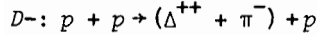
The reactions studied here have the following spin and parity structures in the dissociative process ($a \rightarrow 1 + 2$), ($J_a^P \rightarrow J_1^P + J_2^P$): A- ($0^- \rightarrow 0^+, 0^-$), B- ($0^- \rightarrow 1^-, 0^-$), C- ($1/2^+ \rightarrow 1/2^+, 0^-$) and D- ($1/2^+ \rightarrow 3/2^+, 0^-$).

We choose only one reaction of each type to apply the TCDM. The reactions chosen are respectively:

$$A-: K + p \rightarrow (k+\pi) + p$$



and



We now discuss the results obtained for each of these reactions.

The reactions of type A have the simplest spin and parity structure. The TCM for these reactions may be regeized, what extends the validity of the model beyond the region of resonances in the dissociated subsystem (1+2).

The partial wave amplitudes for the reaction $K + p \rightarrow (k + \pi) + p$ are given by eq. (44). A slope-mass correlation may be observed in the S wave. Fig. (4) shows the theoretical distributions for the S wave in the effective mass ranges $1.25 \leq M_{K\pi} \leq 1.35$ GeV and $1.35 \leq M_{K\pi} \leq 1.50$ GeV respectively.

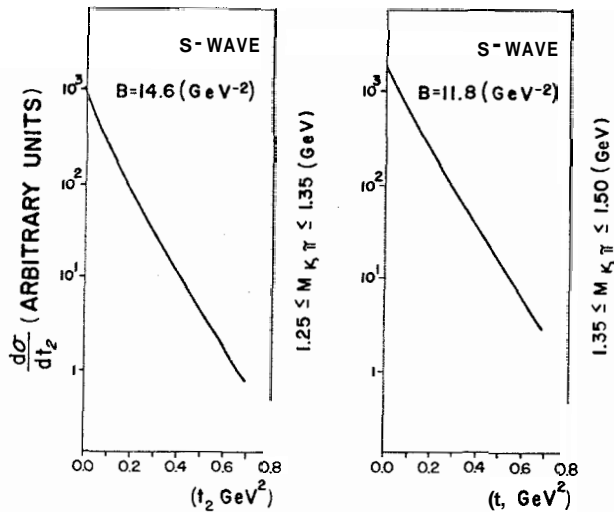


Fig.4 - Partial wave (0^-S) t_2 -distributions and slopes of the reaction $Kp \rightarrow (k\pi)p$, for two effective mass ranges.

The slopes of these distributions, calculated in the interval $0 \leq |t_2| \leq 0.002 \text{ GeV}^2$, are respectively $B = 14.6 \text{ GeV}^{-2}$ and $B = 11.8 \text{ GeV}^{-2}$. These results may be compared with the experimental ones^a, shown in fig. (8).

The parameters of TCDH used to obtain the results above are $\sigma_{\text{tot}}^{\pi N} = 23 \text{ mb}$, $\sigma_{\text{tot}}^{KN} = 20 \text{ mb}$, $\sigma_{\text{tot}}^{K^*N} = 24 \text{ mb}$, $B_{\pi N} = 7 \text{ GeV}^{-2}$, $B_{KN} = 6.5 \text{ GeV}^{-2}$ and $B_{K^*N} = 6.5 \text{ GeV}^{-2}$.

The reaction of type B studied here is $K + p \rightarrow (K^* + \pi) + p$. The helicity amplitudes and the partial wave amplitudes are given by eqs. (23) and (52) respectively.

A slope mass correlation may be observed in the S and P waves. In figs. (5,6,7) we see the distributions for 1^+S and 0^-P waves, restricted by $M=0$, in the effective mass ranges $1.04 \leq M_{K^*\pi} \leq 1.20 \text{ GeV}$, $1.20 \leq M_{K^*\pi} \leq 1.35 \text{ GeV}$ and $1.35 \leq M_{K^*\pi} \leq 1.50 \text{ GeV}$.

The slopes of these distributions calculated in the interval $0 \leq |t_2| \leq 0.02 \text{ GeV}^2$, are given in those figures.

The results for the two higher mass intervals may be compared with the experimental distributions^b and slopes of fig. (8).

The TCDM parameters used to find these experimental slopes are $\sigma_{\text{tot}}^{\pi N} = 22 \text{ mb}$, $\sigma_{\text{tot}}^{K^*N} = 18 \text{ mb}$, $\sigma_{\text{tot}}^{KN} = 21 \text{ mb}$, $B_{\pi N} = 9.0 \text{ GeV}^{-2}$, $B_{K^*N} = 4.5 \text{ GeV}^{-2}$ and $B_{KN} = 3.0 \text{ GeV}^{-2}$.

As may be observed in fig. 5, there exists a strong interference in the 0^-P wave, whose slope is much higher than that of the 1^+S wave. As a consequence of that interference there appears a dip in the 0^-P wave. The dip moves slowly to higher values of $|t_2|$ as $M_{K^*\pi}$ increases.

It must be remembered however that in the mass intervals where the data are given, mainly in the higher ones, there exist $K^*\pi$ resonances.

The dip in the 0^-P wave, predicted by the model, is not seen in the data. Possibly it is covered by resonance effects, or the large errors near $t_2 = -0.3 \text{ GeV}^2$ do not permit to observe the dip.

The reaction of type C, $p + p \rightarrow (n + \pi^+) + p$, allows an excellent test for the TCDM. This reaction has the best data among the DDR. A clear slope-mass- $\cos \theta^{\text{GJ}}$ correlation may be observed in these data. This reaction has some spin complications. However the TCDM may be reggeized

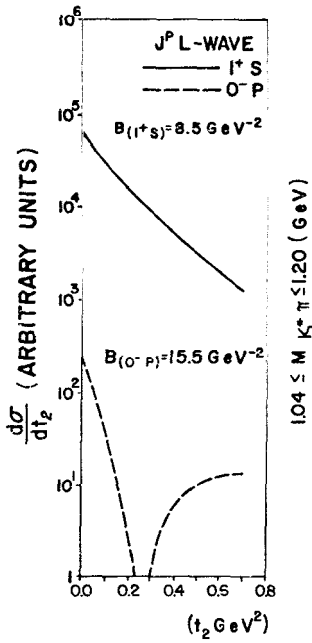


Fig.5 - (1^+S) and (0^-P) partial wave distributions and slopes of the reaction $K_p \rightarrow (K\pi)_p$, in the effective mass range $1.04 \leq M_{K^*\pi} \leq 1.20$ (GeV).

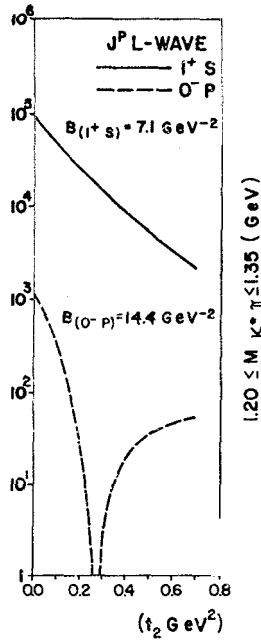


Fig.6 - The same as fig. (5) for $1.20 \leq M_{K^*\pi} \leq 1.35$ (GeV).

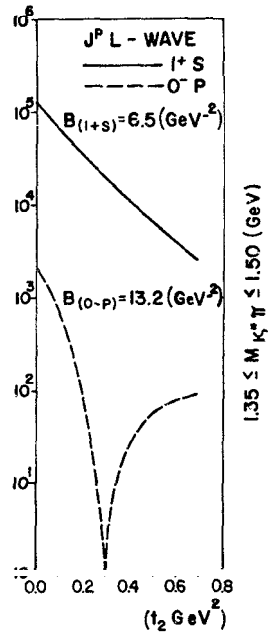


Fig.7 - The same as fig. (5) for $1.35 \leq M_{K^*\pi} \leq 1.50$ (GeV).

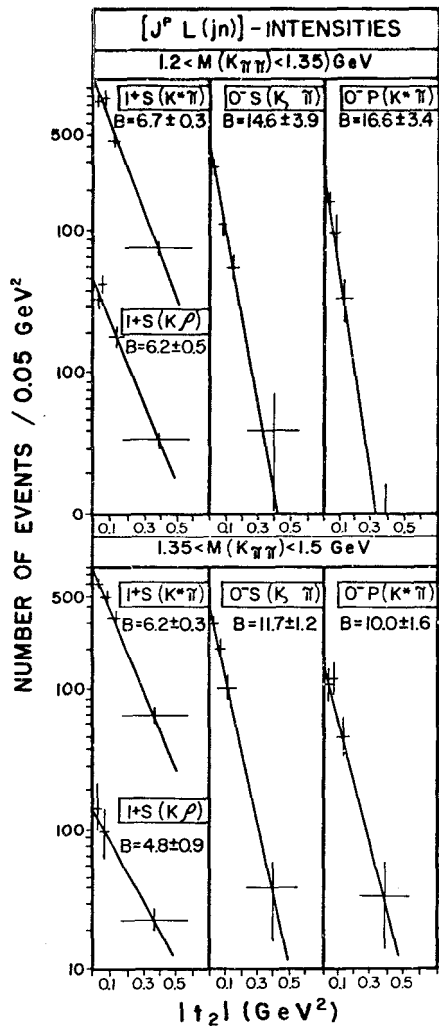


Fig.8 - Experimental results of the partial wave cross sections for the reactions $Kp \rightarrow (k\pi)p - (0^-S)$ and $Kp \rightarrow (K^*\pi)p - (1^+S \text{ and } 0^-P)$, in two effective mass range⁸.

and dualized. Two parametrizations have been obtained for the dualized TCDM. The dual resonance parametrization (DRP) is obtained according to the Veneziano ansatz. We cannot expect that the theoretical mass spectrum fits well the experimental one with this rigid parametrization.

A more flexible parametrization to describe the resonances is the dual reggeized Deck parametrization. In this case the Veneziano functions are replaced by their Regge limits.

The fits of these parametrizations to the data are shown in figs. (9) to (16). The values of the (TCDM) parameters (which are the same for the two cases) are $\sigma_{\text{tot}}^{\pi p} = 25$ mb, $\sigma_{\text{tot}}^{np} = 30$ mb, $\sigma_{\text{tot}}^{pp} = 40$ mb, $B_{\pi p} = 10 \text{ GeV}^{-2}$, $B_{np} = B_{pp} = 9 \text{ GeV}^{-2}$ and $h = 0.3 \text{ GeV}$.

The total mass spectrum, fig. (9), fixes the overall normalizations for the two parametrizations. Fig. (10) shows the $d\sigma/dt_2$ distributions for some windows in $M_{n\pi}$ and $\cos \theta^{\text{GJ}}$. These windows appear in fig. (II), where the zeros of the amplitudes, determined by eqs. (29), are located. Fig. (12) shows the net diffractive slope (B) as a function of the effective mass and the good fitting of the slope predicted by the DRP.

There is a satisfactory agreement of the parametrizations with the $\cos \theta^{\text{GJ}}$ and ϕ^{GJ} distributions, shown in fig. (13). The dualized TCDM reproduces well the turnover of the $\cos \theta^{\text{GJ}}$ distributions at $\cos \theta^{\text{GJ}} = +1$.

Although there are no experimental results to be confronted with, it is interesting to see how the slope mass correlation appears in partial waves. Figs (14,15,16) show the S, P and D waves distributions, restricted by $M = \lambda_{\alpha}$. It may be seen that the strongest interferences occur in the P and D waves, in which there appear dips and turnovers.

Another reaction, of the same type, which is very well described by the dualized TCDM is $p + p \rightarrow (\Lambda + K^+) + p$. See figures (17-21) taken from references 1c, where the comparison with the experimental data was made.

The reaction of type D analyzed here, $p + p \rightarrow (\Delta^{++} + \pi^-) + p$, has helicity amplitudes and partial wave amplitudes given in reference 1d. The complexity of these amplitudes does not permit to derive simple equations to determine the positions of possible zeros. But the numerical calculations of $d\sigma/dt_2$ show that there exists slope-mass corre-

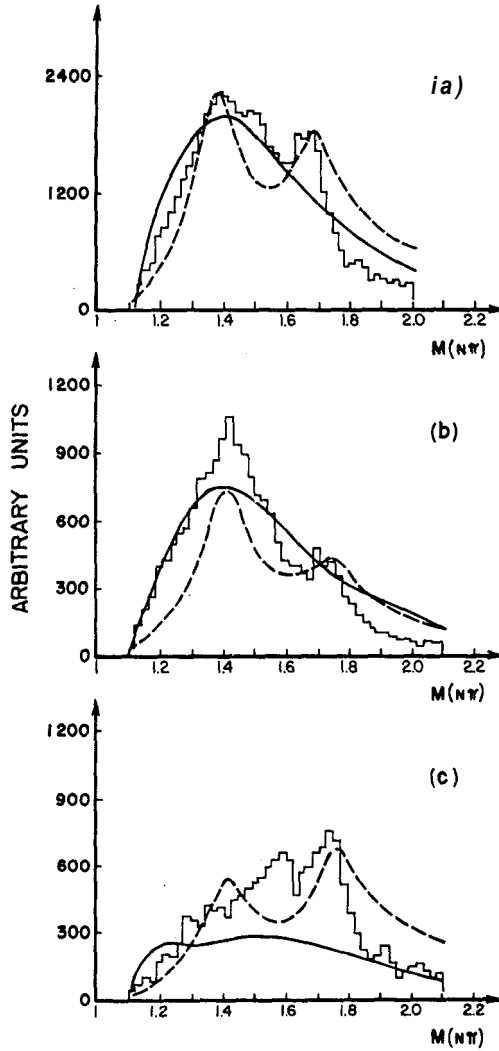


Fig.9 - Effective mass ($M_{N\pi}$) distributions of the reaction $Np \rightarrow (N\pi)p$ for (a) $-0.1 < t_2 < 0.02$; (b) $-0.08 < t_2 < -0.02$ and (c) $-1.0 < t_2 < -0.2$. The full line represents the dual Deck parametrization and the dotted line represents the dual resonance parametrization.

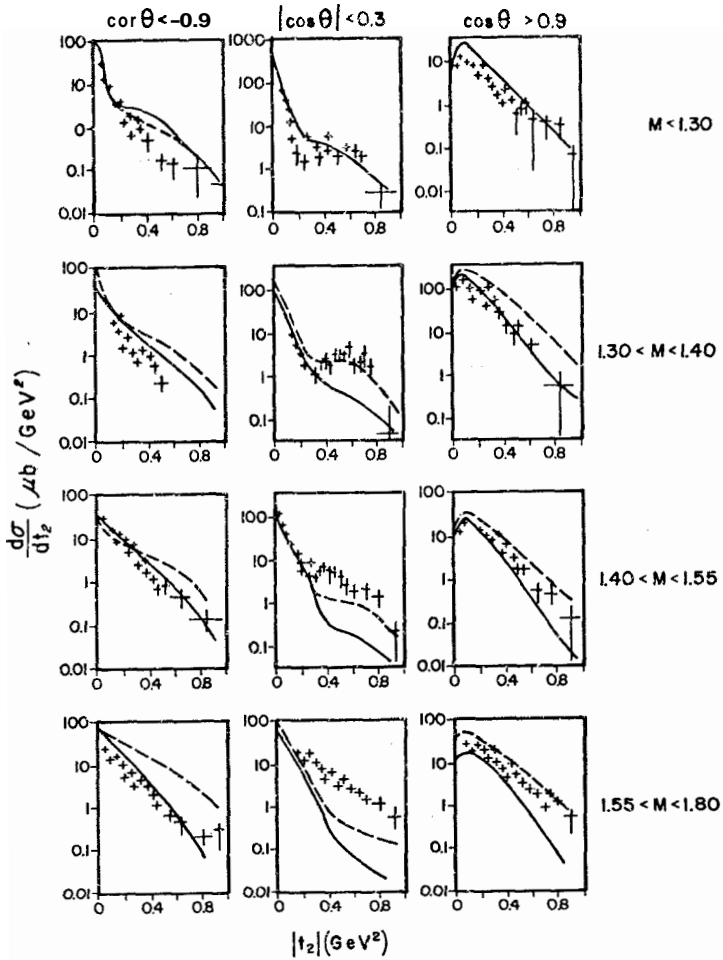


Fig.10 - t_2 distributions integrated in several regions of $M_{N\pi}$ and $\cos \theta_{GJ}$.

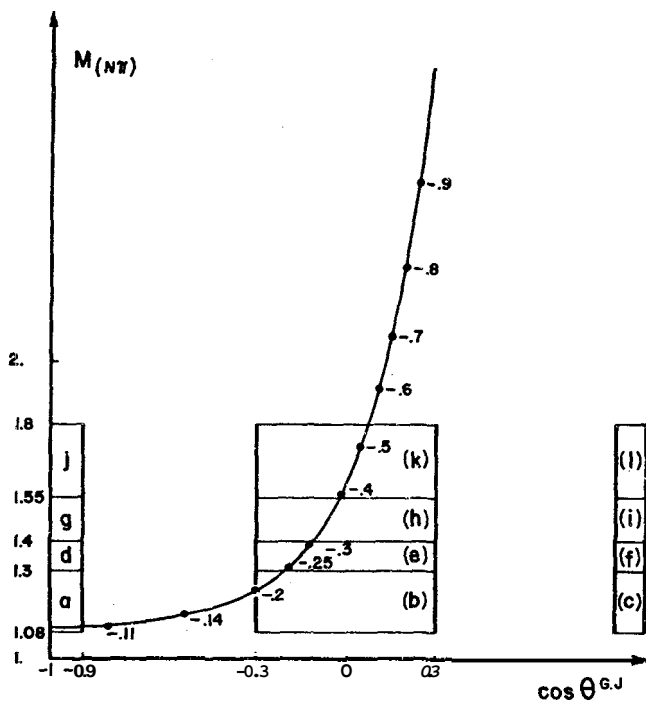


Fig.11 - The location of the zero of the amplitude for $Np \rightarrow (N\pi)p$, as a function of $\cos \theta^{GJ}$, $M_{N\pi}$ and t_2 . The rectangles labelled from (a) to (l) are the regions in $\cos \theta^{GJ}$ and $M_{N\pi}$ in which the t_2 distributions of fig. (10) are integrated.

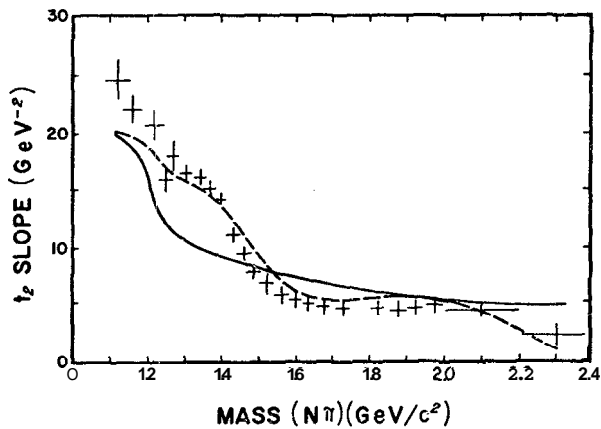


Fig.12 - The t_2 slope as a function of $M_{N\pi}$.

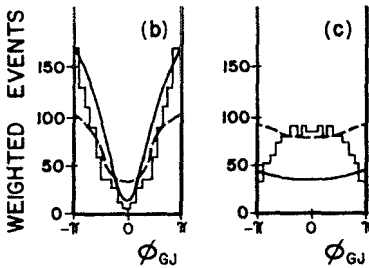
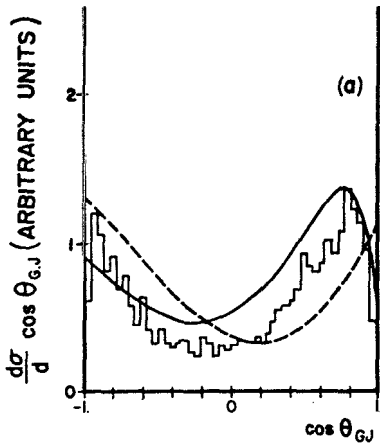


Fig.13 - (a) $\cos \theta_{GJ}$ distribution for $1.08 < M_{N\pi} < 1.4$ (GeV) and $-0.23 < t_2 < 0$.
 (b) ϕ_{GJ} distribution for $1.2 < M_{N\pi} < 1.375$ (GeV), $-0.2 < t_2 < -0.02$ and $0.8 < \cos \theta_{GJ} < 1$.
 (c) The same as (b) except

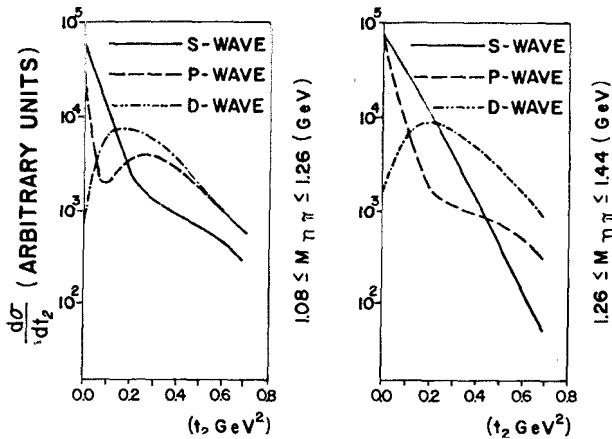


Fig.14 - S, P and D partial wave t_2 distributions for the reaction $Np \rightarrow (N\pi)p$ integrated in two effective mass range, and restricted to $(M = \lambda_a)$.

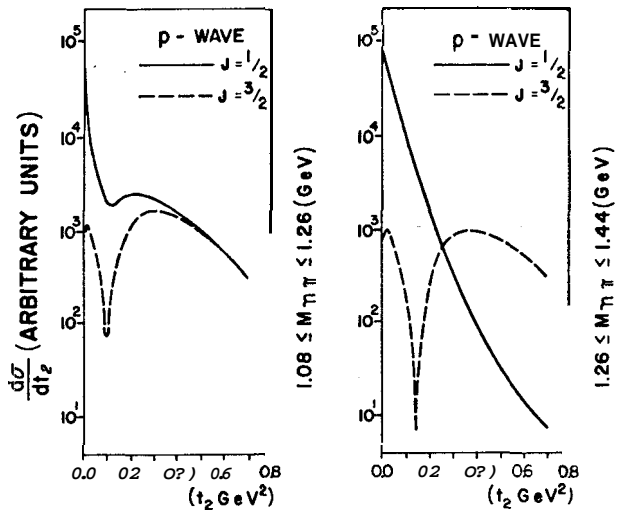


Fig.15 - $P_{(J=1/2)}$ and $P_{(J=3/2)}$ partial wave t_2 distributions.

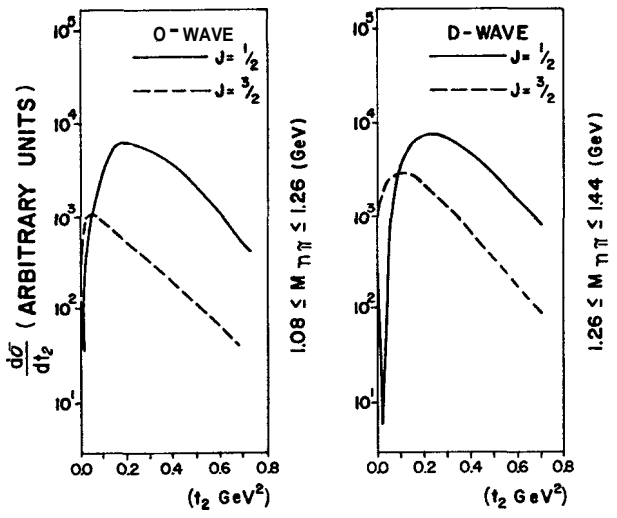


Fig.16 - $D_{(J=3/2)}$ and $D_{(J=5/2)}$ partial wave t_2 distributions.

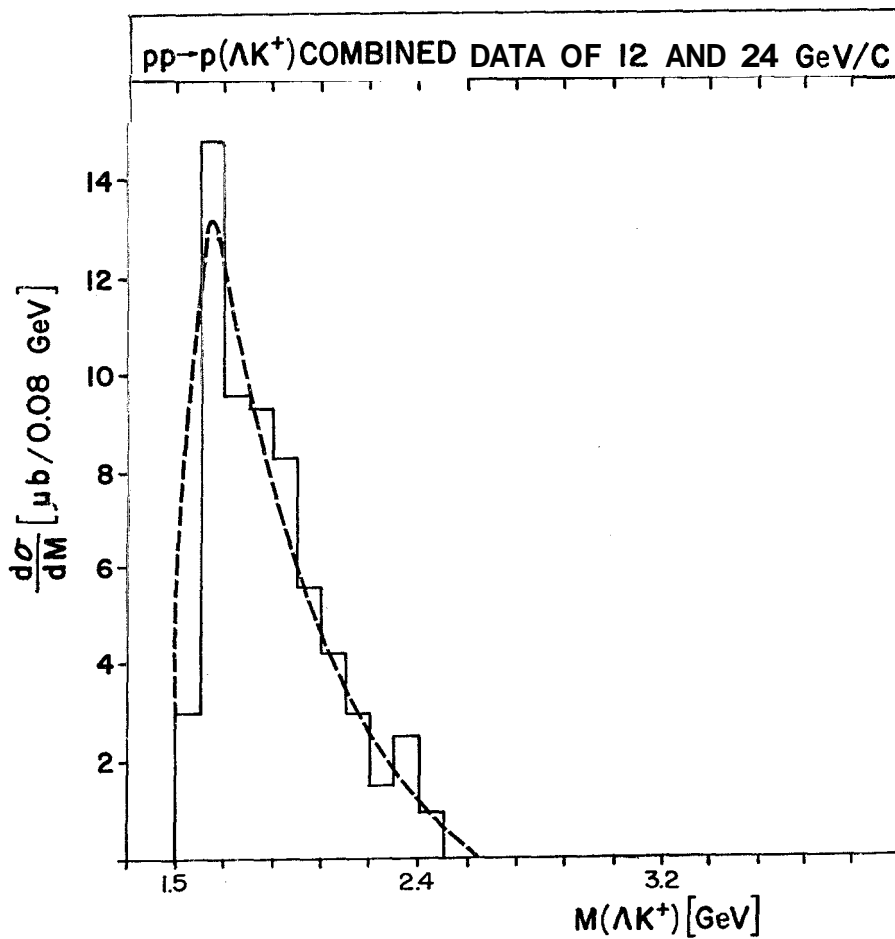


Fig.17 - The mass distribution of the (ΛK^+) system. The full line shows the results of the (TCDM)^{1c}.

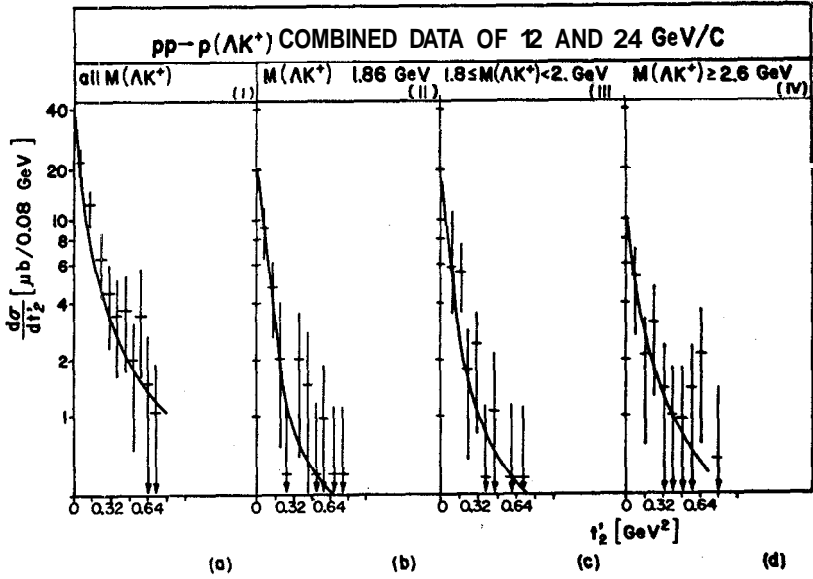


Fig.18 - $d\sigma/dt_2$ distributions for various $M(\Lambda K^+)$ intervals, integrated over all $\cos \theta_{GJ}$ and ϕ_{GJ} . (a) for all $M(\Lambda K)$ masses, (b) for $1.61 \leq M(\Lambda K) \leq 1.8$ GeV, (c) for $1.8 \leq M(\Lambda K) \leq 2.0$ GeV, (d) for $2.0 \leq M(\Lambda K) \leq 2.5$ GeV.

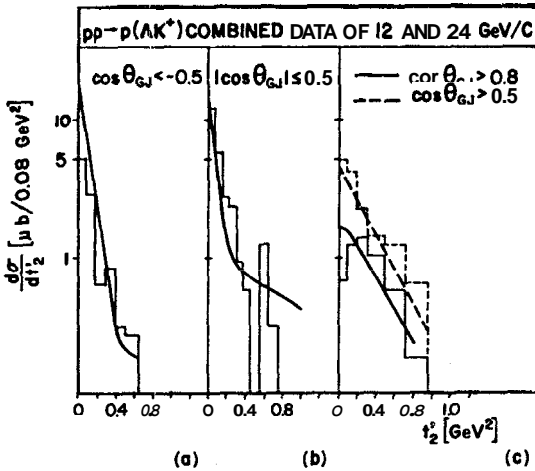


Fig.19 - $d\sigma/dt_2$ distributions for some $\cos \theta_{GJ}$ regions, for all masses of ΛK^+ system and integrated over all ϕ_{GJ} . (a) in the interval $\cos \theta_{GJ} < -0.5$; (b) for $|\cos \theta_{GJ}| \leq 0.5$; (c) $\cos \theta_{GJ} \geq 0.8$ (full line), $\cos \theta_{GJ} \geq 0.5$ (dotted line).

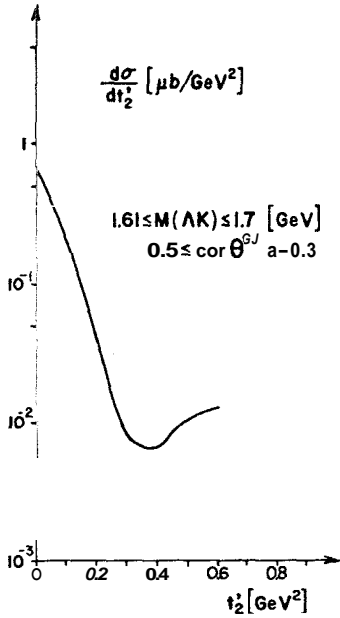


Fig. 20-a

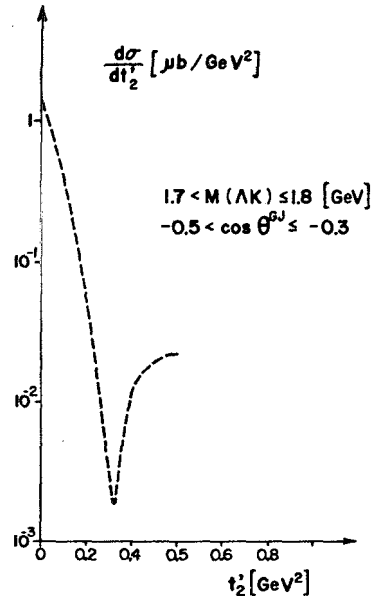


Fig. 20-b

Fig.20 - Theoretical $d\sigma/dt_2$ distributions calculated by (TCDDM). (a) In the intervals $1.61 \leq M(\Lambda K) \leq 1.7$ (GeV) and $-0.5 \leq \cos \theta_{GJ} \leq -0.3$. (b) In the intervals $1.7 < M(\Lambda K) < 1.8$ (GeV) and $-0.5 < \cos \theta_{GJ} < -0.3$.

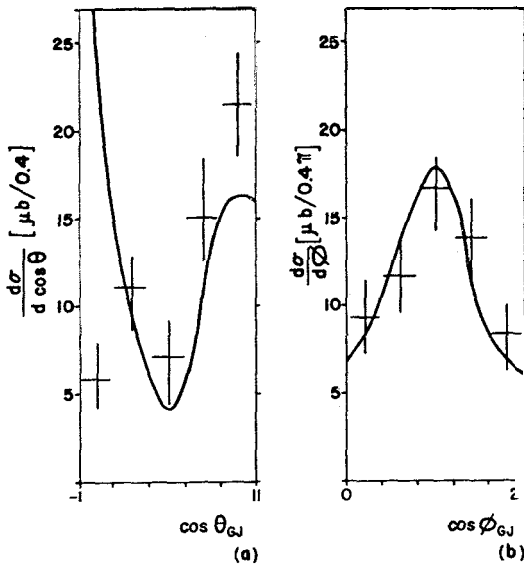


Fig.21 - Gottfried-Jackson angle distributions for all masses $M(\Lambda K)$ and for $0 < |t_2| < 1$. (a) $\cos \theta_{GJ}$ distribution integrated over all ϕ_{GJ} . (b) ϕ_{GJ} distribution integrated over all $\cos \theta_{GJ}$.

lations in the distributions for that reaction. In fig. (22) we see that the slope decreases as the effective mass increases. Fig. (23) shows how the slope depends on the effective mass and on the $\cos \theta^{\text{GJ}}$ intervals

The set of parameters of TOCM used in these calculations are $\sigma_{\text{tot}}^{\pi N} = 25$ mb, $\sigma_{\text{tot}}^{NN} = 40$ mb, $\sigma_{\text{tot}}^{N\Delta} = 50$ mb, $B_{\pi N} = 10 \text{ GeV}^{-2}$, $B_{NN} = 9 \text{ GeV}^{-2}$ and $B_{N\Delta} = 8 \text{ GeV}^{-2}$, and the slopes are calculated in the interval $0 \leq |t_2| \leq 0.02 \text{ GeV}^2$.

The best way to see the slope mass correlation in this reaction is to look at the partial wave distributions. It must be remembered that the partial wave distributions are here restricted by the condition $M = A_a$. This condition has the advantage of simplifying the calculations and is enough to exhibit a possible slope-mass-partial wave correlation.

In fig. (24) we see the S, P and D wave distributions for two effective mass intervals. The S wave shows a strong interference, with a dip at $t_2 \simeq -0.35 \text{ GeV}$.

The examination of each amplitude $A(L_J^P)_{1/2}$, for P and D wave distributions, allows us to seek for interference structures not seen in fig. (24).

Fig. (25) shows the $A(P_{1/2}^+)_{1/2}$, $A(P_{3/2}^+)_{1/2}$ and $A(P_{5/2}^+)_{1/2}$ distributions. Among these, the $A(P_{3/2}^+)_{1/2}$ is the one that shows the strongest interference, with a dip at $t_2 \simeq -0.1 \text{ GeV}^2$.

The relative normalization in fig. (25) shows that the partial wave $A(P_{1/2}^+)_{1/2}$ is two orders of magnitude larger than $A(P_{3/2}^+)_{1/2}$, where the strongest interference occurs. For this reason the total P wave distributions, showed in fig. (24), do not present dips.

The D wave spectrum for each J, i.e., the $A(D_{1/2}^-)_{1/2}$, $A(D_{3/2}^-)_{1/2}$, $A(D_{5/2}^-)_{1/2}$ and $A(D_{7/2}^-)_{1/2}$ wave distributions are shown in fig. (26). We remark that only the $A(D_{1/2}^-)_{1/2}$ and $A(D_{7/2}^-)_{1/2}$ waves present dips at $t_2 \simeq -0.6 \text{ GeV}^2$ and $t_2 \simeq -0.4 \text{ GeV}^2$ respectively. The total D wave distribution, showed in fig. (24) does not present dips because all the contributions from different J values are added.

The net slopes for each wave, calculated in the interval $0 \leq |t_2| \leq 0.02 \text{ GeV}$, are shown in tables 1 and 2. In table 2 we remark that all waves, but $P_J = 3/2$, present an expected mass-slope-partial wave correlation, that is, the slope decreases as the effective mass $M_{\Lambda\pi}$ increases.

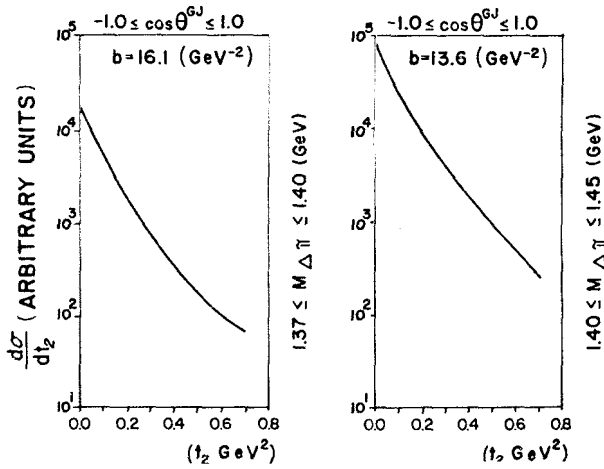


Fig.22 - t_2 distributions and slopes, for reaction $pp \rightarrow (\Delta^{++}\pi^-)p$, integrated in two effective mass ranges.

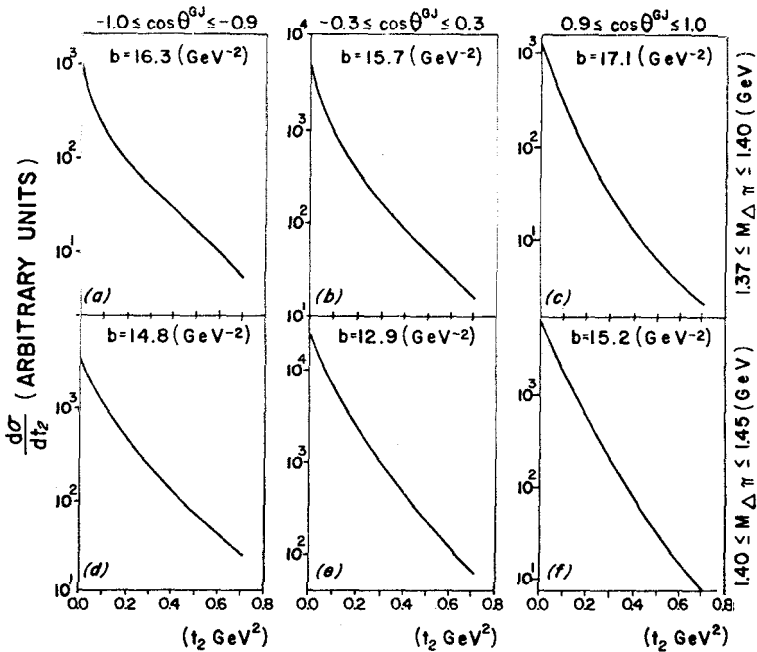
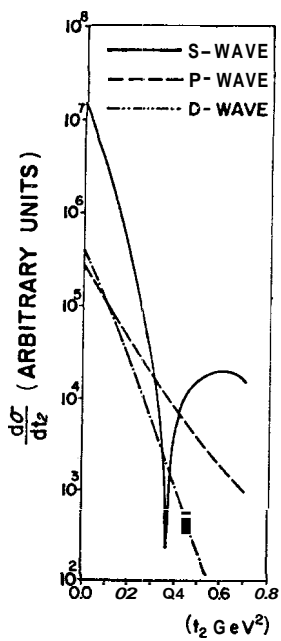
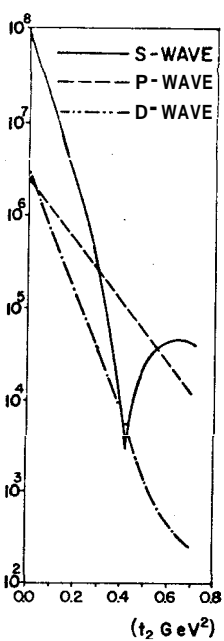


Fig.23 - t_2 distributions and slopes for $pp \rightarrow (\Delta^{++}\pi^-)p$, integrated in two intervals of $M_{\Delta\pi}$ and three intervals of $\cos \theta_{GJ}$.

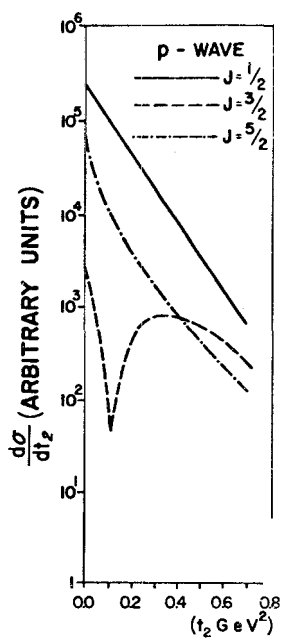


$1.37 \leq M_{\Delta\pi} \leq 1.00$ (GeV)

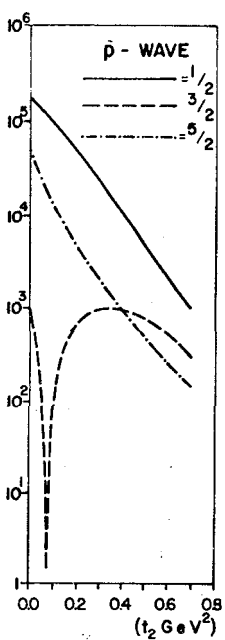


$1.40 \leq M_{\Delta\pi} \leq 1.45$ (GeV)

Fig. 24 - S, P and D partial wave t_2 distributions, restricted to $(M = \lambda_\alpha)$



$1.37 \leq M_{\Delta\pi} \leq 1.40$ (GeV)



$1.40 \leq M_{\Delta\pi} \leq 1.45$ (GeV)

Fig. 25 - $P^{(J=1/2)}$, $P^{(J=3/2)}$ and $P^{(J=5/2)}$ partial wave t_2 distributions, restricted to $(M = \lambda_\alpha)$.

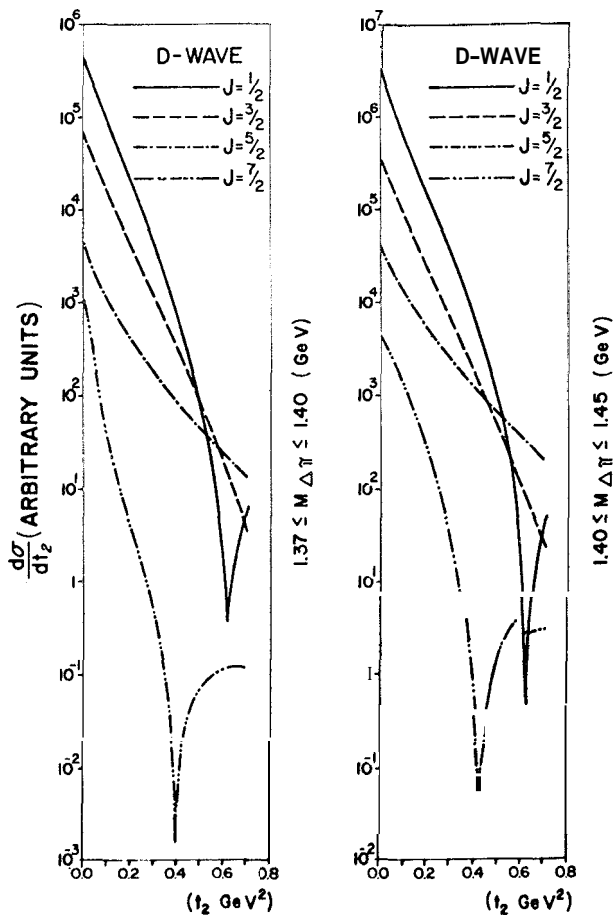


Fig. 26 - $D_{(j=1/2)}$, $D_{(j=3/2)}$, $D_{(j=5/2)}$ and $D_{(j=7/2)}$ partial wave t_2 distributions, restricted to $(M = \lambda_\alpha)$.

The abnormal behaviour of the $P_{J=3/2}$ happens because the zero occurs for smaller $|t_2|$ when s_1 increases.

The reactions of type A and B are analysed with combined data from experiments at 10, 14 and 16 GeV incident K^- momenta. And for the reactions of type C and D the data come from experiments at 12 and 24 GeV incident proton momenta. It was observed that there is no significant variation of the cross sections in the energy intervals analysed.

L	$1.37 \leq M_{\Delta\pi} \leq 1.40 \text{ GeV}$	$1.40 \leq M_{\Delta\pi} \leq 1.45 \text{ GeV}$
S	$B = 19.5$	$B = 17.4$
P	$B = 9.7$	$B = 7.3$
D	$B = 16.7$	$B = 16.1$

Table 1 - Values in GeV^{-2} of the slopes corresponding to the curves $d\sigma/dt_2$ shown at fig. 24.

L	J	$1.37 \leq M_{\Delta\pi} \leq 1.40 \text{ GeV}$	$1.40 \leq M_{\Delta\pi} \leq 1.45 \text{ GeV}$
P	$1/2$	$B = 7.1$	$B = 4.5$
	$3/2$	$B = 24.2$	$B = 33.2$
	$5/2$	$B = 22.8$	$B = 18.1$
ρ	$1/2$	$B = 17.2$	$B = 16.4$
	$3/2$	$B = 13.4$	$B = 13.0$
	$5/2$	$B = 18.9$	$B = 13.2$
	$7/2$	$B = 43.2$	$B = 34.7$

Table 2 - Values in GeV^{-2} of the slopes for each wave with well defined L and J values, shown in figs. 25 and 26.

APPENDIX A

This appendix contains a **summary** of the kinematlcal variables and expresslons used in this paper.

The DDR $a + b \rightarrow (1+2) + 3$ may be represented as in flg. (1), and the TODM which describes these reactlons has the diagrams of flg. (2).

The four-momenta corresponding to the **external** lines are $p_i (i = a, b, 1, 2, 3)$ and for the **internal** lines we define

$$q = p_a - p_1, \quad k = p_a - p_2 \quad \text{and} \quad p = p_1 + p_2 \quad (\text{A.1})$$

At the diffractive vertlces the following four-momenta are used

$$P = (p_1 + k)/2, \quad Q = (p_2 + q)/2 \quad (\text{A.2})$$

$$K = (p_a + p)/2, \quad R = (p_b + p_3)/2$$

The invariants constructed with these 4-vectors are

$$\begin{aligned} s &= (p_a + p_b)^2, \quad s_1 = (p_1 + p_2)^2, \quad s_2 = (p_2 + p_3)^2 \\ s_3 &= (p_1 + p_3)^2, \quad t_1 = (p_a - p_1)^2, \quad u_1 = (p_a - p_2)^2 \\ t_2 &= (p_b - p_3)^2 \end{aligned} \quad (\text{A.3})$$

The energies E_i and the momenta $|\vec{p}_i| (i=a,b,1,2,3)$ are defined in the Gottfried-Jackson frame for $\vec{p}_1 + \vec{p}_2 = 0$ the 1 + 2 rest system, see flg. 27. The expresslons of E_i and $|\vec{p}_i|$ are given by

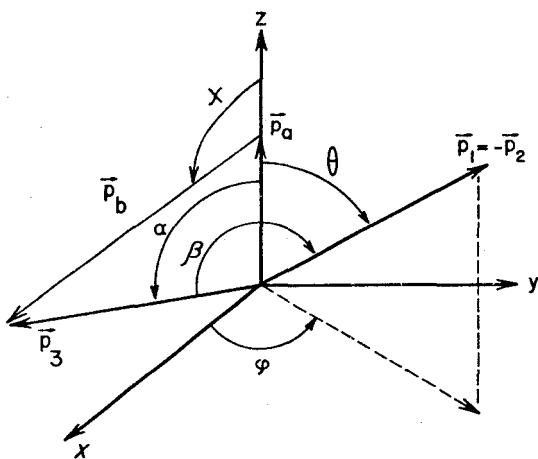


Fig. 27 - Gottfried - Jackson coordinates for $R12 (\vec{p}_1 + \vec{p}_2 = 0)$.

$$\begin{aligned}
E_a &= (s_1 + m_a^2 - t_2) / 2\sqrt{s_1} \quad , \quad E_b = (s_1 - m_a^2 - m_3^2 + t_2) / 2\sqrt{s_1} \\
E_1 &= (s_1 + m_1^2 - m_2^2) / 2\sqrt{s_1} \quad , \quad E_2 = (s_1 + m_2^2 - m_1^2) / 2\sqrt{s_1} \\
E_3 &= (s - s_1 - m_3^2) / 2\sqrt{s_1} \quad , \quad |\vec{p}_a| = \lambda^{1/2}(s_1, m_a^2, t_2) / 2\sqrt{s_1} \\
|\vec{p}_b| &= \lambda^{1/2}(s_1, m_b^2, t_{a3}) / 2\sqrt{s_1} \quad , \quad |\vec{p}_3| = \lambda^{1/2}(s_1, m_3^2, s) / 2\sqrt{s_1}
\end{aligned}$$

and

$$|\vec{p}_1| = |\vec{p}_2| = \lambda^{1/2}(s_1, m_1, m_2^2) / 2\sqrt{s_1} \quad (\text{A.4})$$

where

$$t_{a3} = s_1 - s - t_2 + m_a^2 + m_b^2 + m \quad (\text{A.5})$$

and $\lambda(x, y, z)$ is defined by

$$\lambda(x, y, z) = x^2 + y^2 + z^2 - 2(xy + xz + yz) \quad (\text{A.6})$$

The angular coordinates for the momenta are

$$\vec{p}_1 = \vec{p}_1(\theta, \phi) \quad , \quad \vec{p}_b = \vec{p}_b(\chi, 0) \quad \text{and} \quad \vec{p}_3 = \vec{p}_3(\alpha, 0) \quad (\text{A.7})$$

The angles in GJS are related by

$$\cos \beta = \cos \alpha \cos \theta + \sin \alpha \sin \theta \cos \phi \quad (\text{A.8})$$

High energy approximation (HEA)

These approximations correspond to

$$s, s_2, s_3 \gg s_1, |t_1|, |u_1|, |t_2|, m_i^2 \quad (i=a, b, 1, 2, 3) \quad (\text{A.9})$$

Using eq. (A.9) we obtain

$$2Q.R \simeq s_2 \quad , \quad 2P.R \simeq s_3 \quad , \quad 2K.R \simeq s \quad (\text{A.i0})$$

$$\cos \alpha \simeq -(s_1 - m_a^2 + t_2) / \lambda^{1/2}(s_1, m_a^2, t_2)$$

$$\sin a \simeq 2\sqrt{s_1} \sqrt{-t_2} / \lambda^{1/2} (s_1, m_a^2, t_2) \quad (\text{A.11})$$

$$s_2 \simeq s(E_2 + |\vec{p}_1| \cos \beta) / \sqrt{s_1} \quad \text{and} \quad s_3 \simeq s(E_1 - |\vec{p}_1| \cos \beta) / \sqrt{s_1} \quad (\text{A.12})$$

For very small values of $|t_2|$ eq. (A.8) becomes

$$\cos \beta \simeq -\cos \theta + (2\sqrt{s_1} \sqrt{-t_2} / (s_1 - m_a^2)) \sin \theta \cos \phi \quad (\text{A.13})$$

then, carrying into eq. (A.12) we obtain

$$s_2 \simeq s(E_2 - |\vec{p}_1| \cos \theta) / \sqrt{s_1} + (2s |\vec{p}_1| \sqrt{-t_2} / (s_1 - m_a^2)) \sin \theta \cos \phi$$

and

$$s_3 \simeq s(E_1 + |\vec{p}_1| \cos \theta) / \sqrt{s_1} - (2s |\vec{p}_1| \sqrt{-t_2} / (s_1 - m_a^2)) \sin \theta \cos \phi \quad (\text{A.14})$$

In the same approximations we have

$$(t_1 - m_2^2) \simeq -(s_1 - m_a^2)(E_2 - |\vec{p}_1| \cos \theta) / \sqrt{s_1} \quad (\text{A.15})$$

and

$$(u_1 - m_1^2) \simeq -(s_1 - m_a^2)(E_1 + |\vec{p}_1| \cos \theta) / \sqrt{s_1}$$

From eqs. (A.14) and (A.15) we obtain

$$\frac{s_3}{u_1 - m_1^2} \simeq -\frac{s}{s_1 - m_a^2} \left[1 - \frac{2|\vec{p}_1| \sqrt{s_1} \sqrt{-t_2} \sin \theta \cos \phi}{(s_1 - m_a^2)(E_1 + |\vec{p}_1| \cos \theta)} \right] \quad (\text{A.16})$$

and

$$\frac{s_2}{t_1 - m_2^2} \simeq -\frac{s}{s_1 - m_a^2} \left[1 + \frac{2|\vec{p}_1| \sqrt{s_1} \sqrt{-t_2} \sin \theta \cos \phi}{(s_1 - m_a^2)(E_2 - |\vec{p}_1| \cos \theta)} \right]$$

and at the limit $t_2 = 0$, we have the relation

$$\frac{s_2}{t_1 - m_2^2} \simeq \frac{s_3}{u_1 - m_1^2} \simeq -\frac{s}{s_1 - m_a^2} \quad (\text{A.17})$$

For a three particles final state reaction the cross-section is given by

$$d\sigma = C \int \frac{\lambda^{1/2}(s_1, m_1^2, m_2^2)}{s_1} ds_1 dt_2 d \cos \theta d\phi |A|^2 \quad (\text{A.18})$$

where

$$C = 1/(2^{10} \pi^4 \lambda(s, m_a^2, m_b^2))$$

APPENDIX B

In this appendix we collect some results useful for the projection into partial waves of the helicity amplitudes, obtained through the TCDM, for the DDR.

neglecting the spin structure of (~~bP3~~) vertex, due to the factorization property, the helicity amplitude, given by the TCDM for the DDR $\mathbf{a} + \mathbf{b} \rightarrow (1+2) + 3$, in the GJS, making use of the Jacob-Wick convention, has an explicit phase

$$A_{\lambda_1 \lambda_2 \lambda_a}(s, s_1, t_2; \theta, \phi) = e^{-i(\lambda - \lambda_a)\phi} A_{\lambda_1 \lambda_2 \lambda_a}(s, s_1, t_2; \theta, \phi) \quad (\text{B.1})$$

where $h = \lambda_1 - \lambda_2$.

The helicity amplitudes for total angular momentum J of the dissociated subsystem (1+2) and its projection M , on the incident beam direction \vec{p}_a , and normality \pm , are given by

$$A_{\lambda_1 \lambda_2 \lambda_a}^{JM\pm}(s, s_1, t_2) = [(2J+1)/8\pi]^{1/2} \int d\Omega e^{-i(M-\lambda_a)\phi} \times \left\{ d_{M\lambda}^J(\theta) \tilde{A}_{\lambda_1 \lambda_2 \lambda_a}(\theta, \phi) \pm N_{12} d_{M, -\lambda}^J(\theta) \tilde{A}_{-\lambda_1, -\lambda_2, \lambda_a}(\theta, \phi) \right\} \quad (\text{B.2})$$

where

$$N_{12} = \eta_1 \eta_2 (-1)^{\delta_1 + \delta_2 - v_{12}} \quad (\text{B.3})$$

In the above expression η_1 and η_2 , and δ_1 and δ_2 are the intrinsic parities and spins of the particles 1 and 2 respectively; $v_{12} = 0$ for integer J and $v_{12} = 1/2$ for half integer J .

The parities of the amplitudes are given by

$$P = \pm (-1)^{J - v_{12}} \quad (\text{B.4})$$

For $\lambda_1 = \lambda_2 = 0$ instead of eq. (8.2) we have

$$A_{00, \lambda_\alpha}^{JM, N_{12}} = ((2J+1)/4\pi)^{1/2} \int d\Omega e^{-i(M-\lambda_\alpha)\phi} a_{M0}^J(\theta) \chi_{00\lambda_\alpha}(\theta, \phi) \quad (\text{B.5})$$

From parity conservation we obtain the relation

$$A_{-\lambda_1, -\lambda_2, -\lambda_\alpha}^{J, -M, \pm} = \eta(-1)^{M-\lambda_\alpha} A_{\lambda_1 \lambda_2 \lambda_\alpha}^{JM, \pm} \quad (\text{B.6})$$

where

$$\eta = \eta_1 \eta_2 \eta_\alpha (-1)^{\delta_1 + \delta_2 - \delta_\alpha} \quad (\text{B.7})$$

The amplitudes in eq. (8.2) also satisfy

$$A_{-\lambda_1, -\lambda_2, \lambda_\alpha}^{JM, \pm} = \pm N_{12} A_{\lambda_1 \lambda_2 \lambda_\alpha}^{JM, \pm} \quad (\text{B.8})$$

The amplitudes for well defined J, M , orbital angular momentum L , spin $\vec{s} = \vec{s}_1 + \vec{s}_2$ and normality (\pm) , of the subsystem 1+2 are given by

$$A_{(L, s) \lambda_\alpha}^{JM, \pm} = ((2L+1)/(2J+1))^{1/2} \sum_{\lambda_1 \lambda_2} C_{0 \lambda \lambda}^{L \delta J} C_{\lambda_1, -\lambda_2, \lambda}^{\delta_1 \delta_2 \delta} A_{\lambda_1 \lambda_2 \lambda_\alpha}^{JM, \pm} \quad (\text{B.9})$$

where $C_{0 \lambda \lambda}^{L \delta J}$ and $C_{\lambda_1, -\lambda_2, \lambda}^{\delta_1 \delta_2 \delta}$ are the Clebsh-Gordan coefficients. In the cases for which $s_2 = 0, \delta = \delta_1$, the amplitudes in eq. (B.9) become

$$A_{(L) \lambda_\alpha}^{JM, \pm} = ((2L+1)/(2J+1))^{1/2} \left[1 \pm N_{12} (-1)^{J-L-\delta_1} \right] \sum_{|\lambda_1|} C_{0 |\lambda_1| |\lambda_1|}^{L \delta_1 J} A_{|\lambda_1| \lambda_\alpha}^{JM, \pm} \quad (\text{B.10})$$

From the eqs. (6.6) and (B.8) we obtain

$$A_{(L), -\lambda_\alpha}^{J, -M, \pm} = \pm N_{12} \cdot \eta(-1)^{M-\lambda_\alpha} A_{(L) \lambda_\alpha}^{J, M, \pm} \quad (\text{B.11})$$

REFERENCES

1. a) G.Cohen-Tannoudji, A.Santoro and M.Souza, N.Physics B125, 445 (1977); b) G.Cohen Tannoudji, D.Levy and M.Souza -N. Phys. B 129, 286 (1977); c) A.Endler, M.A.R.Monteiro, A.Santoro and M. Souza, Z. für Physik C7, 137 (1981); d) A.C.B.Antunes, A.F.S.Santoro and M.H. G.Souza, Rev.Bras. de Física 13, 415 (1983) and 13, 601 (1983).
2. G.Alberi and G.Goggi, Phys. Rep. 74, 1 (1981).
3. a) D.R.O. Morrison, P. Lett. 22, 528 (1966) and P. Rev.165, 1699
b) V.N.Gribov-Yad. Fiz.5, 197 (1967); Sov. J. Nucl. Phys. 5, 138 (1967).
4. G.Otter, Acta Physica Polonica B3, 809 (1972).
5. P.D.B. Collins and F.D.Gault, Nucl. Phys. B112, 483 (1976).
6. a) S.D.Drell and K.Hida, Phys.Rev.Lett. 199 (1961); b) R. T. Deck Phys. Rev. Lett.13, 169 (1964); c) M.Ross and Y.Y.Yam, Phys. Rev. Lett. 19, 546 (1967).
7. a) C.Broll, Thesis - Université de Paris 7 (1976); b) J. Biel *et al.* Phys. Rev. Lett. 36, 504, 507 (1976); c) See references In 1a above.
8. G. Otter *et al.*, Nucl. Phys. B106, 77 (1976).

Resumo

Neste artigo apresentamos um conjunto de novos resultados de Reações de Dissociação Difractiva, no contexto do Modelo Deck a Três Componentes. Estes novos resultados são confrontados com outros recentemente publicados para apresentar uma visão geral do modelo, suas previsões e comparações com resultados experimentais. Dois tipos de amplitudes e correlações são observadas. A correlação inclinação difractiva-massa-cos θ_{GJ} e a inclinação difractiva-massa-ondas parciais.